Plasma Sources Sci. Technol. **9** (2000) 507–516. Printed in the UK PII: S0963-0252(00)15594-X

Lecture notes on radio-frequency discharges, dc potentials, ion and electron energy distributions

W J Goedheer

FOM-Institute for Plasmaphysics, PO Box 1207, 3430 BE Nieuwegein, The Netherlands

E-mail: goedheer@rijnh.nl

Received 1 October 1999, in final form 28 June 2000

Abstract. These notes are meant as a first introduction into the physics of capacitively coupled radio-frequency discharges for people that are about to start or have just started research involving gas discharges. The scope is limited to the basic electrical characteristics and to the behaviour of the positive ions and electrons in the discharge.

Introduction

Capacitively coupled radio-frequency (RF) discharges are often used for etching and deposition of thin solid layers on a substrate attached to one of the electrodes. Important application areas are the semiconductor industry and the fabrication of thin-film solar cells and thin-film transistors [1–5]. RF discharges are especially useful when the layer to be treated is a semiconductor or an isolator; then a dc discharge current cannot be sustained and an alternating current is required. The frequency of this alternating current must be so high that the charged particles created in one half of the RF cycle are not lost when the current goes through zero. The frequencies thus needed are typically above 50 kHz. Commonly used is 13.56 MHz and in very high-frequency (VHF) discharges frequencies up to more than 100 MHz are used. RF discharges are usually operated at low pressures, typically 5–150 Pa, the lower end of this range is used for etching and the higher end for deposition. Discharge parameters are, roughly, a density of 10^{15}–10^{17} m^{-3} and an electron temperature of 1–4 eV. These parameters, of course, depend on the power dissipated (1–300 W, approximately) and on the gas mixture that is used. In many gases, negative ions are formed; here we focus on electropositive discharges. The distance between the planar electrodes in experiments is 1–10 cm and the radius is, typically, 10 cm. A rough outline of an RF reactor is shown in figure 1.

For etching purposes, the substrate is mostly attached to the smallest (powered) electrode; for deposition to the grounded electrode. This choice is related to the difference in the energy of positive ions bombarding the surface, as will be discussed in sections 1 and 2 of these notes.

An important advantage of RF discharges over other discharges discussed in other parts of this course is that they are relatively easy to scale up to larger dimensions.

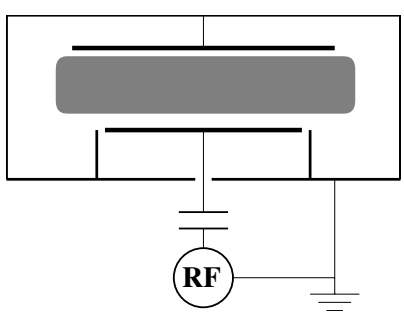

Figure 1. Schematic diagram of the geometry of a planar RF discharge; not drawn are the gas inlet and the vacuum pumps.

A drawback is that the energy of the bombarding ions is coupled to the dissipated power, which hampers control of the ion bombardment. A way to overcome this is by changing the frequency of the power source. At the higher frequencies a lower voltage is required at the same power.

An important aspect of RF discharges is that they are far from equilibrium. The electrons in the central quasi-neutral plasma reach a much higher average energy than the ions. The electrons cannot share the energy they gain from the electric field with the much heavier ions and neutrals because the collision frequency is not high enough and because the energy transfer in an elastic collision is proportional to the (small) mass ratio. The electrons loose their energy mainly in inelastic collisions, such as excitation, dissociation, and ionization. This implies that the first step in the plasma chemistry of RF discharges, the dissociation of the feed gas molecules into radicals, is totally driven by the electrons. This makes the electron energy distribution function a crucial parameter in the discharge behaviour. The behaviour of the electron energy distribution function is discussed in section 3 of these notes.

0963-0252/00/040507+10$30.00

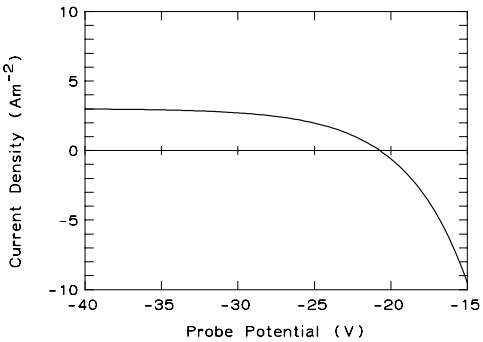

Figure 2. A current–voltage characteristic for a planar probe in a Maxwellian plasma with $N_\infty = 10^{16}$ m^{-3}, $M_+ = 40M_H$, and $kT_e = 4$ eV.

1. Electrical characteristics

1.1. The planar probe

Consider a plane probe with unit area, facing a semi-infinite discharge with a Maxwellian plasma of singly-charged positive ions and electrons with a density N_∞ and electron temperature T_e. If the potential of the probe is negative with respect to the discharge, electrons will be pushed away from it and positive ions will be attracted to it. This leads to a charge separation and to the generation of a space charge sheath which separates the quasi-neutral bulk plasma from the probe. The simplest theory of this sheath, assuming mono-energetic positive ions and a Maxwellian electron energy distribution, shows that the ion current to the probe is constant and equal to the so-called Bohm current, while the electron current is the thermal current weakened by the Boltzmann factor:

$$I_+ = 0.606eN_\infty \left(\frac{kT_e}{M_+}\right)^{1/2} \tag{1a}$$

$$I_e = -\frac{1}{4}eN_\infty \left(\frac{8kT_e}{\pi m_e}\right)^{1/2} \exp\left(\frac{eV}{kT_e}\right). \tag{1b}$$

This leads to a current–voltage characteristic as shown in figure 2.

If the probe is capacitively coupled and no external potential is applied, it will acquire a negative charge such that the net current becomes zero; its potential at that point is the so-called floating potential. The application of a RF signal to the probe, however, will change the value of the average potential. Figure 3 shows the current flowing to the probe during one RF cycle when an alternating potential of 4 V is added to the floating potential in the characteristic of figure 2. Because of the nonlinearity in the current–voltage characteristic, the probe will collect more electrons than positive ions and is charged further still, until a new average potential is reached where the net current is again zero. The generation of a bias voltage to fulfill the requirement of a zero net current is an important phenomenon in RF discharges, as will be shown in the next paragraph. Applying an RF bias to a substrate in a so-called high-density plasma that is generated using microwaves or an inductive source, for instance, provides a way to control the energy of the ions bombarding the substrate. This is required, in particular, for profile control during etching of structures in the sub-micrometre range [3].

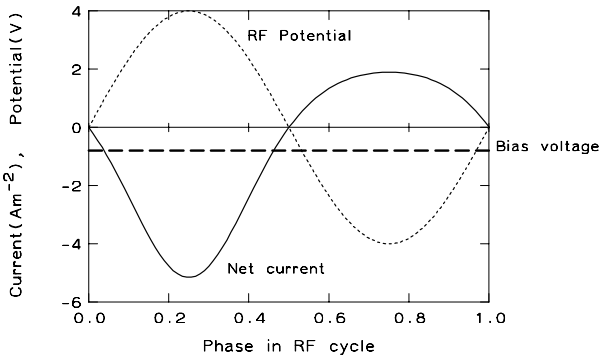

Figure 3. Current against phase of an RF signal applied to a floating probe. Current equilibrium can only be reached by the generation of an extra bias voltage.

1.2. The RF discharge as a system of planar probes

The voltage–current characteristic of the planar probe can be used to describe the electrical features of the RF discharge at low frequencies. Low frequencies in this case means that we do not consider the displacement current generated by the variation of the charge on the probe.

Consider again a Maxwellian plasma as before, but now two probes are inserted, at a distance so large that the boundary layers do not overlap and a quasi-neutral plasma with density N_∞ and electron temperature T_e is formed in between. One of the probes is grounded, the other one is capacitively coupled to a RF power source. Since, in practice, the discharge chamber is also grounded, the grounded probe will usually have a larger area than the powered probe. If we take $V = 0$ in the quasi-neutral central part, the current to each of the probes is given by

$$I_{1,2}(t) = A_{1,2}eN_\infty\left[0.606\left(\frac{kT_e}{M_+}\right)^{1/2} - \frac{1}{4}\left(\frac{8kT_e}{\pi m_e}\right)^{1/2} \exp\left(\frac{eV_{1,2}(t)}{kT_e}\right)\right] \tag{2}$$

where A_i is the area of probe i and V_i its potential. Since the probes are part of a closed circuit (figure 4), Kirchoff's law demands that the currents to each probe are opposite, so

$$A_1\left[0.606\left(\frac{kT_e}{M_+}\right)^{1/2} - \frac{1}{4}\left(\frac{8kT_e}{\pi m_e}\right)^{1/2} \exp\left(\frac{eV_1(t)}{kT_e}\right)\right] = -A_2\left[0.606\left(\frac{kT_e}{M_+}\right)^{1/2} - \frac{1}{4}\left(\frac{8kT_e}{\pi m_e}\right)^{1/2} \exp\left(\frac{eV_2(t)}{kT_e}\right)\right]. \tag{3}$$

The capacitive coupling demands that the current averaged over one RF cycle must be zero:

$$\overline{I_{1,2}(t)} = \frac{1}{2\pi}\int_0^{2\pi} I_{1,2}\,\mathrm{d}\omega t = 0. \tag{4}$$

The potentials V_2 and V_1 of the probes are coupled by the applied RF voltage and possibly a dc bias due to the charging of the capacitor:

$$V_2(t) - V_1(t) = V_0 \sin(\omega t) + V_{dc}. \tag{5}$$

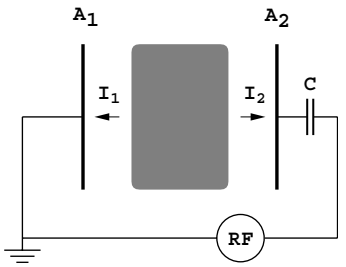

Figure 4. The RF discharge as a system of two planar probes.

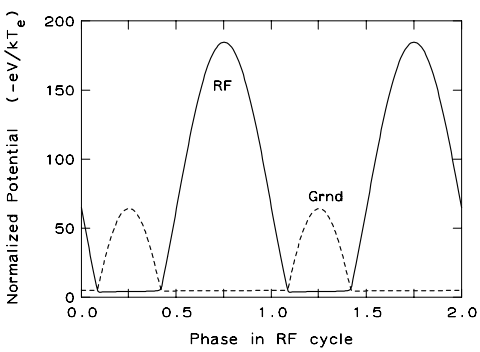

Figure 5. The normalized potential drop over the space charge sheaths in an RF discharge in argon ($M_+ = 40$), with an area ratio $\alpha = 2$, at a frequency of 100 kHz. The normalized RF voltage and dc bias are 120 and 59.7, respectively. Note that two cycles are shown.

Let us now introduce the following parameters and normalized quantities:

$$\alpha = A_1/A_2 \qquad \beta = \frac{0.606(kT_e/M_+)^{1/2}}{\frac{1}{4}(8kT_e/\pi m_e)^{1/2}} \approx 1.52\left(\frac{m_e}{M_+}\right)^{1/2}$$

$$\tau = \omega t \qquad \Phi = -\frac{eV}{kT_e}.$$

This reduces the set of equations to

$$\alpha[\beta - \exp(-\Phi_1(\tau))] = -[\beta - \exp(-\Phi_2(\tau))] \tag{6}$$

$$\frac{1}{2\pi}\int_0^{2\pi} \exp(-\Phi_1(\tau))\,\mathrm{d}\tau = \frac{1}{2\pi}\int_0^{2\pi} \exp(-\Phi_2(\tau))\,\mathrm{d}\tau = \beta \tag{7}$$

$$\Phi_2(\tau) - \Phi_1(\tau) = \Phi_0 \sin(\tau) + \Phi_{dc}. \tag{8}$$

The procedure leading to a solution starts by choosing Φ_{dc}; this determines $\Phi_2(\tau)$ and $\Phi_1(\tau)$. From this the average current can be computed, which should be zero. The value of Φ_{dc} for which, indeed, the average current vanishes is obtained iteratively, by means of a Newtonian method.

The results for a reactor with $\alpha = 2$, filled with argon ($M_+ = 40M_H$) and $\Phi_0 = 120$ are presented in figure 5. Note, that the discharge switches between two modes, with a very short transient phase in between. Either electrode 1 repels the electrons and I_1 equals the ion current, while the potential of electrode 2 is sufficiently close to zero to have an electron current matching this ion current ($I_2 = -I_1$), or *vice versa*. Figure 6 shows the currents $I_{1,2}(t)$.

The results above are valid for low frequencies, where the displacement current does not play a significant role. At high

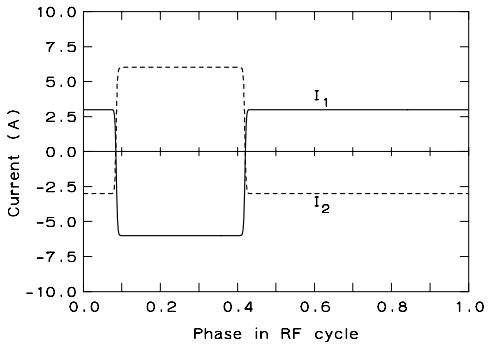

Figure 6. The total current to each electrode for the potential curves of figure 5. Here only one cycle is shown.

frequencies the displacement current cannot be neglected. Its origin is the variation in time of the charge on the electrodes. This charge depends on the potential difference between the quasi-neutral bulk plasma and the electrode. As can be shown from Maxwell's law

$$\vec{\nabla}\cdot\vec{E} = \frac{e}{\epsilon_0}(N_+ - N_e)$$

or

$$\oint \vec{E}\cdot\mathrm{d}\vec{O} = \frac{e}{\epsilon_0}\iiint (N_+ - N_e)\,\mathrm{d}\vec{r} \tag{9}$$

for a rectangular box with one plane in the bulk and one plane in the (perfectly conducting) electrode, the positive space charge in the sheath always equals the negative charge on the electrode. Thus, we have to find an expression for the positive charge in the sheath. The simplest assumption, of course, is a constant ion density and a zero electron density in the sheath and equal ion and electron densities in the bulk. The boundary conditions on the potential are $V = 0$ and $E = 0$ in the bulk ($x = 0$) and $V = V_{el}$ on the electrode, which determines the sheath width, d. Poisson's equation in one dimension

$$\frac{\partial^2 V}{\partial x^2} = -\frac{eN_+}{\epsilon_0} \tag{10}$$

then has the solution

$$V(x) = -\frac{eN_+}{2\epsilon_0}x^2 \tag{11a}$$

$$d = \left(-\frac{2\epsilon_0 V_{el}}{eN_+}\right)^{1/2} \tag{11b}$$

which results in a total charge per unit area

$$Q_{el} = -Q_{sheath} = -eN_+ d = -\sqrt{(-2e\epsilon_0 N_+ V_{el})}^{1/2} \tag{12}$$

and a displacement current, again per unit area,

$$\frac{\partial Q_{el}}{\partial t} = C(V)\frac{\partial V}{\partial t} = -\left(-\frac{e\epsilon_0 N_+}{2V_{el}}\right)^{1/2}\frac{\partial V}{\partial t}. \tag{13}$$

Thus, the contribution of the displacement current can be considered that of a voltage-dependent capacitance. Since the displacement current depends on the integral of the charge density in the sheath, differences between various sheath models (giving different expressions for $C(V_{el})$) are not very

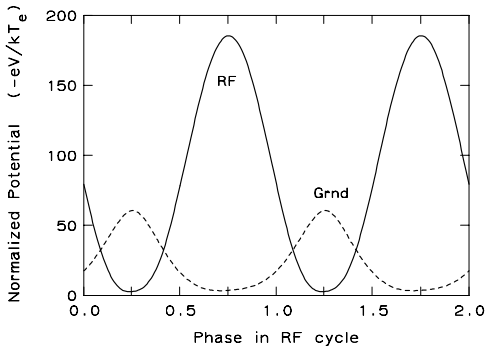

Figure 7. As figure 5, but for a frequency of 13.56 MHz. The normalized dc bias is 62.0.

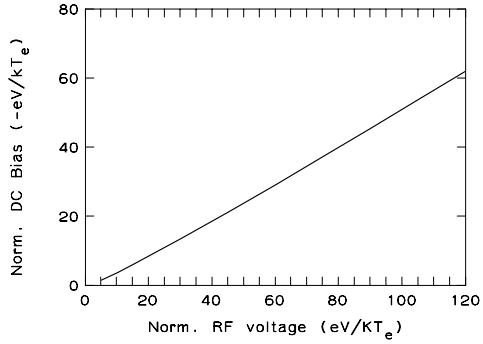

Figure 8. Bias against RF voltage for an area ratio $\alpha = 2$. The frequency is 13.56 MHz.

large [6]. The displacement current has to be added to Kirchoff's law; it does not contribute to the average current since V_{el} is periodic. The current balance to be solved thus becomes

$$A_1\left[0.606\left(\frac{kT_e}{M_+}\right)^{1/2} - \frac{1}{4}\left(\frac{8kT_e}{\pi m_e}\right)^{1/2}\exp\left(\frac{eV_1(t)}{kT_e}\right) - \frac{\partial Q_1}{\partial t}\right]$$
$$= -A_2\left[0.606\left(\frac{kT_e}{M_+}\right)^{1/2} - \frac{1}{4}\left(\frac{8kT_e}{\pi m_e}\right)^{1/2} \times \exp\left(\frac{eV_2(t)}{kT_e}\right) - \frac{\partial Q_2}{\partial t}\right]. \quad (14)$$

Figure 7 shows the influence of the displacement current. All parameters are the same as for figure 5, except the frequency, which is increased to 13.56 MHz. The major difference is that the potential on both electrodes has become much more harmonic.

Assumptions made, in the calculation of both figures 5 and 7, are the neglection of secondary electrons (released from the electrodes due to the ion bombardment) and a time-independent ion density in the sheath. The flux of secondary electrons is proportional to the ion flux (1%, typically) and will lead to a slightly different parameter β in equation (6). At low frequencies, the ion density and the ion flux may vary in time, but certainly at high frequencies this is a minor correction.

It is possible that larger deviations are caused by the fact that the electron and ion current density are not the same at each part of the electrodes. The discharge may, for instance, contract itself in between the electrodes, leaving a less important contribution to the current balance from other grounded parts, such as the cylindrical sidewalls [7].

With the model discussed, we can compute the behaviour of the bias as a function of the applied RF voltage at a fixed ratio α and as a function of α at a fixed value of V_{RF}. Results are given in figures 8 and 9, for discharges operated at a frequency of 13.56 MHz. In conclusion, the double-probe model shows that the sheaths can be considered to consist of an almost linear element, a voltage-dependent capacitance, and a strongly nonlinear element, the combined fluxes of ions and electrons. Obviously, in the case of an applied harmonic potential, this nonlinear element will lead to the generation of higher harmonics in the current flowing through the circuit, and *vice versa* in the potential when a harmonic current is applied for the power generation. Often, the discharge is

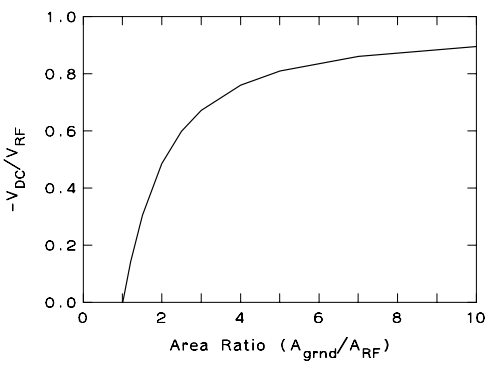

Figure 9. The ratio of the bias and the RF voltage against the area ratio, for a driving voltage $eV_{RF} = 120\,kT_e$. The frequency is 13.56 MHz.

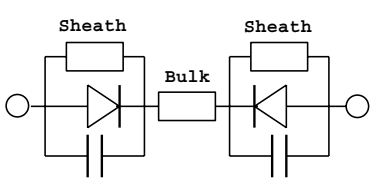

Figure 10. Equivalent circuit of a RF discharge.

represented by a scheme as in figure 10; one has to be aware that the diode is not a real diode, but represents the current–voltage characteristic of the probe and that the capacitance is not a constant, but depends on the voltage.

To match the complex impedance of the RF reactor to the RF power source, a matching network is required. This network will have an influence on the amount of power that actually goes into the plasma [8].

In the case where the applied frequency is so high that the sheath–bulk transition moves at a speed comparable to the average velocity of the electron fluid, the characteristics of the discharge change again. The electrons can be heated significantly by this so-called 'wave-riding' ([4], ch 11).

2. Ion energy distribution functions

2.1. Collisionless ion energy distribution functions

If the applied RF frequency is sufficiently low, the positive ions need only a small fraction of the RF cycle to cross the sheath, and they will reach the electrode with an energy equal

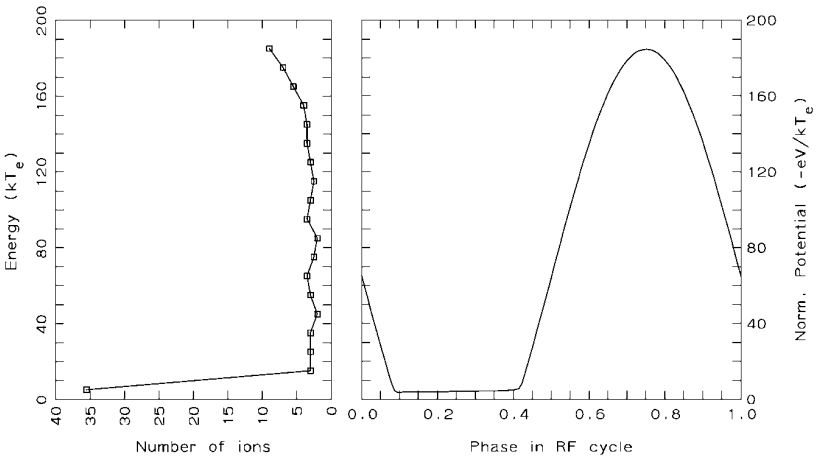

Figure 11. The ion energy distribution at low frequencies.

to the instantaneous potential drop over the sheath. The ion energy distribution function will reflect the time dependence of this potential drop as given in figure 5. This implies that peaks in the energy distribution can be expected where the time derivative of the potential drop is zero. This is illustrated in figure 11.

Things become more complicated at high frequencies. High frequencies in this context means that the ions need much longer than one RF period to transit the sheath. To estimate this transit time, let us again consider the simple sheath model with a constant ion density and no time dependence, so

$$V(x) = -\frac{eN_+}{2\epsilon_0}x^2 \tag{15}$$

as before. If the initial energy of the ions is small (Bohm velocity) and no collisions occur, so the sum of the kinetic energy and the potential energy is constant, the velocity of the ions at position x is

$$\frac{\mathrm{d}x}{\mathrm{d}t} = v_+ = \left(\frac{-2eV(x)}{M_+}\right)^{1/2} = \left(\frac{e^2N_+}{M\epsilon_0}\right)^{1/2}x. \tag{16}$$

The solution is

$$x = x_0\exp(\omega_{pi}t) \tag{17a}$$

with

$$\omega_{pi} = \left(\frac{e^2N_+}{M\epsilon_0}\right)^{1/2} \tag{17b}$$

as the ion plasma frequency. Thus, ω_{pi} is a measure for the transit time and a high frequency means $\omega_{RF} \gg \omega_{pi}$.

For a somewhat more accurate calculation of the spatial dependence of the electric field, which accounts for the spatial dependence of the ion density, we assume that there are no electrons in the sheath ($\exp(eV/kT_e) \ll 1$) and that the ions are collisionless. The absence of electrons also implies that the production of ions in the sheath is neglected. The continuity of the ion flux, Γ_+, implies

$$\Gamma_+(x) = \Gamma_0 = N_+(0)v_+(0) = N_+(x)v_+(x). \tag{18}$$

If we take the initial energy of the ions to be γkT_e (Bohm, cf equation (1a), would imply a choice $\gamma = 0.5$), conservation of energy implies $v_+(x) = v_0(1+\Phi(x)/\gamma)^{1/2}$, where $\Phi(x) = -eV(x)/kT_e$, so

$$N_+(x) = \frac{N_+(0)}{(1+\Phi(x)/\gamma)^{1/2}}. \tag{19}$$

Poisson's equation for the electric potential then reads

$$\frac{\partial^2\Phi(x)}{\partial x^2} = \frac{e^2}{\epsilon_0 kT_e}N_+(0)\frac{1}{(1+\Phi/\gamma)^{1/2}} = \frac{1}{\lambda_D^2(1+\Phi/\gamma)^{1/2}} \tag{20}$$

where λ_D is the Debye length in the bulk of the discharge. The solution of Poisson's equation, obtained after neglecting 1. compared to ϕ/γ, multiplication with $\mathrm{d}\Phi/\mathrm{d}x$, and partial integration, is

$$\Phi^{3/4}(x) = \frac{3}{2}\gamma^{1/4}\frac{x}{\lambda_D}. \tag{21}$$

The boundary condition at the electrode, $\Phi(d) = \Phi_{el}$, introduces a relation between γ, Φ_{el}, and d:

$$\gamma = \left[\frac{2\lambda_D}{3d}\right]^4\Phi_{el}^3. \tag{22}$$

This determines the initial ion energy and the initial ion current:

$$eN_+(0)v_+(0) = \frac{4}{9}eN_+(0)\left(\frac{2kT_e}{M_+}\right)^{1/2}\frac{\lambda_D^2}{d^2}\Phi_{el}^{3/2}. \tag{23}$$

This is the so-called Child–Langmuir or space charge limited current density [4].

The results of figure 7 show that the behaviour of V_{el} in time can be described reasonably well with a harmonic function and an offset. With the spatial dependence obtained above, the sheath potential reads

$$V(x,t) = V_0(1+\lambda\sin(\omega t))\left(\frac{x}{d}\right)^{4/3} \tag{24a}$$

$$E(x) = -\frac{4V_0}{3d}(1+\lambda\sin(\omega t))\left(\frac{x}{d}\right)^{1/3}. \tag{24b}$$

The equation of motion of ions moving in the sheath is therefore

$$\frac{\mathrm{d}^2x}{\mathrm{d}t^2} = \frac{4eV_0}{3M_+d}[1+\lambda\sin(\omega t)]\left(\frac{x}{d}\right)^{1/3}. \tag{25}$$

If λ is small [9] or if the frequency is sufficiently high, the path of the ions will be close to that corresponding to the average acceleration:

$$\frac{\mathrm{d}^2x}{\mathrm{d}t^2} = \frac{4eV_0}{3M_+d}\left(\frac{x}{d}\right)^{1/3} \tag{26a}$$

$$\left(\frac{x(t)}{d}\right) = \left[\frac{1}{3d}\left(\frac{2eV_0}{M_+}\right)^{1/2}\right]^3(t-t_0)^3 \tag{26b}$$

with t_0 the time at which the ion enters the sheath. The insertion of this path into the original equation of motion yields

$$\frac{\mathrm{d}^2x}{\mathrm{d}t^2} = \frac{4\sqrt{2}}{9}\omega^2 d\left(\frac{eV_0}{M\omega^2d^2}\right)^{3/2}[1+\lambda\sin(\omega t)](\omega t-\omega t_0). \tag{27}$$

Time integration results in the velocity:

$$\begin{aligned}\frac{\mathrm{d}x}{\mathrm{d}t} &= \frac{4\sqrt{2}}{9}\omega d\left(\frac{eV_0}{M_+\omega^2d^2}\right)^{3/2}\int_{\omega t_0}^{\omega t}(\tau-\tau_0)(1+\lambda\sin\tau)\,\mathrm{d}\tau \\ &= \frac{4\sqrt{2}}{9}\omega d\left(\frac{eV_0}{M_+\omega^2d^2}\right)^{3/2}\left[\frac{1}{2}(\omega t-\omega t_0)^2\right. \\ &\quad \left.+\lambda(\sin\omega t-\sin\omega t_0)-\lambda(\omega t-\omega t_0)\cos\omega t\right].\end{aligned} \tag{28}$$

At the electrode, the ion energy reached at time t_1 is

$$\begin{aligned}&\frac{16}{81}eV_0\left(\frac{eV_0}{M\omega^2d^2}\right)^2\left[\frac{1}{2}(\omega t_1-\omega t_0)^2+\lambda(\sin\omega t_1-\sin\omega t_0)\right. \\ &\quad \left.-\lambda(\omega t_1-\omega t_0)\cos\omega t_1\right]^2.\end{aligned} \tag{29}$$

The time of arrival at the electrode is again obtained from the 'average' motion

$$\omega t_1-\omega t_0 = 3\omega d\left(\frac{M_+}{2eV_0}\right)^{1/2}. \tag{30}$$

If the ion needs many cycles to transit the sheath, the second term enclosed in the square brackets in the final energy can be neglected compared to the other two, and we are left with

$$\begin{aligned}W &= eV_0\left[1-\frac{2\lambda}{3\omega d}\left(\frac{2eV_0}{M_+}\right)^{1/2}\cos\omega t_1\right]^2 \\ &\approx eV_0\left[1-\frac{4\lambda}{3\omega d}\left(\frac{2eV_0}{M}\right)^{1/2}\cos\omega t_1\right].\end{aligned} \tag{31}$$

With a constant flux of ions entering the sheath,

$$\Gamma = \frac{\mathrm{d}N_{tot}}{\mathrm{d}t} = \frac{\mathrm{d}N_{tot}}{\mathrm{d}W}\frac{\mathrm{d}W}{\mathrm{d}t} \tag{32}$$

the distribution function becomes

$$f(W) = \frac{\mathrm{d}N_{tot}}{\mathrm{d}W} = \frac{\Gamma}{\omega\Delta W}\left[1-\left(\frac{2}{\Delta W}\right)^2(W-eV_0)^2\right]^{-1/2}. \tag{33}$$

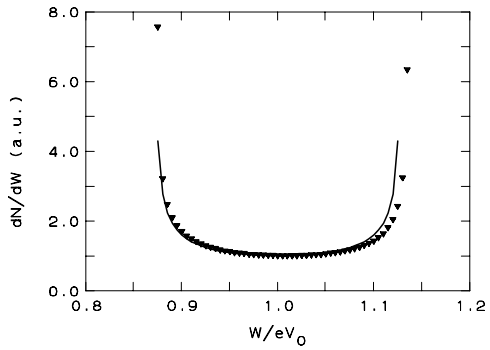

Figure 12. The ion energy distribution at high frequencies. The parameters are a frequency of 15 MHz, a modulation factor of 0.95, an amplitude of 500 V, a mass of 40 M_H and a sheath width of 5 mm. The full curve is the approximation and the symbols are computed without neglection of small terms.

This is a saddle-shaped distribution with a width

$$\Delta W = |W_{max}-W_{min}| = \frac{8\lambda eV_0}{3\omega d}\left(\frac{2eV_0}{M_+}\right)^{1/2}. \tag{34}$$

In figure 12, an example of a high-frequency distribution function is given. If we compare this distribution with that of figure 11, we see that the peaks, which correspond to situations where $\mathrm{d}V_{el}/\mathrm{d}t = 0$, have moved toward each other; the energies corresponding to the minimum and maximum potential drop can no longer be reached. In reality, the contribution of small terms that were thrown away will render the distribution asymmetric (the symbols in figure 12). Also, the finite resolution of the energy analyser will smear out the distribution function. Nevertheless, comparing the measured (collisionless) distributions with the simple saddle shape above reveals important information on the space charge sheath. If the ion mass is known, the average energy combined with the width of the distribution gives the thickness of the sheath.

2.2. Influence of collisions

Ions moving in the space charge sheath will collide mainly with the background neutral gas; three kinds of collisions are important.

- Elastic collisions will lead to deviations from a perpendicular incidence on the electrode and to the loss of the kinetic energy. For anisotropic etching, the ions should arrive perpendicular to the substrate. To minimize the effect of collisions, etching is usually performed at relatively low gas pressures.
- Symmetric charge exchange collisions will lead to a complete loss of the energy of the ion, which is taken over by a neutral of the same species:

$$\mathrm{A}^+_{fast} + \mathrm{A}_{slow} \rightarrow \mathrm{A}_{fast} + \mathrm{A}^+_{slow}.$$

- Chemical reactions or asymmetric charge exchange will remove the ion involved and a different ion may be formed. If chemical reactions or asymmetric charge exchange change the identity of the ion considered, things are simple: they do not contribute to the energy

distribution function. Of course, if these processes capture ions of a certain energy range, the shape of the distribution function may be affected.

More easily observable are the effects of the other types of collisions. Elastic collisions, for instance, will simply lead to a tail of lower energies, with a shape that depends on the scattering differential cross section and the mass of the collision partner. Symmetric charge exchange and the generation of new (cold) ions in the sheath also have a pronounced effect on the form of the distribution function. Their influence is visible through a number of additional peaks [10]. Figure 13 shows simulated distribution functions in which the total mean free path is kept constant, but the relative contributions of the elastic collisions and the charge exchange are varied from almost no charge exchange (top) to almost no elastic collisions (bottom) [11]. Experimentally obtained distribution functions are compared with calculations in figure 14, under various conditions [12]. The mechanism which generates the peaks is the oscillating front of the electron density. If an ion is stopped at a certain position and at that moment the potential of the electrode is low enough (in absolute value), the electron density front may be in between the ion position and the electrode. The ion is then in the quasi-neutral part and feels no electric field. It waits, until the electron front has moved back and is then suddenly accelerated again. Thus, the ions are bunched and each successive RF cycle creates a new bunch. The bunch with the lowest energy was created one cycle before arrival, that with the next lowest energy two cycles previously, and so on. The average energy of each bunch corresponds to the average potential drop the ions have experienced. For an assumed average potential distribution, the relation between the transit time $t - t_0$, the average energy $e\langle V\rangle$, and the distance x/d is known; the value of the average potential of the quasi-neutral bulk can be obtained from the peak of a collisionless ion. With these data, the average potential profile can be reconstructed and part of the structure of the sheath can be unravelled. The behaviour of the average net charge density and the thickness of the sheath will, for instance, give information on the capacitance of the sheath.

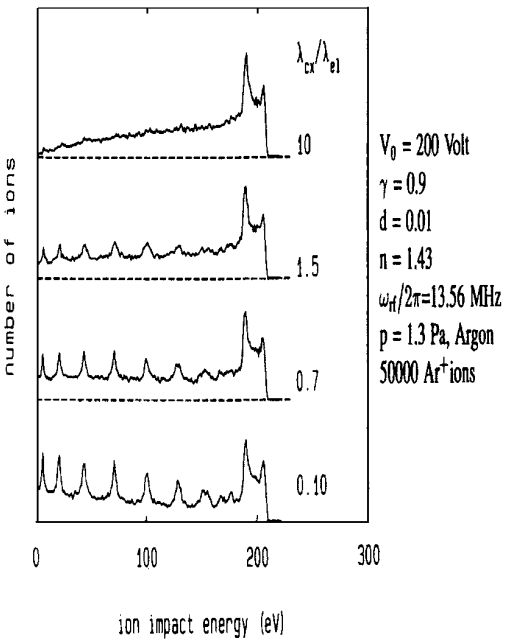

Figure 13. Changes in the ion energy distribution function when the relative contribution of elastic collisions is changed from ten times (top) to one tenth (bottom) of that of the charge exchange. The distributions are obtained from a Monte Carlo calculation for a sheath with parameters given at the right-hand side. Illustration from [11].

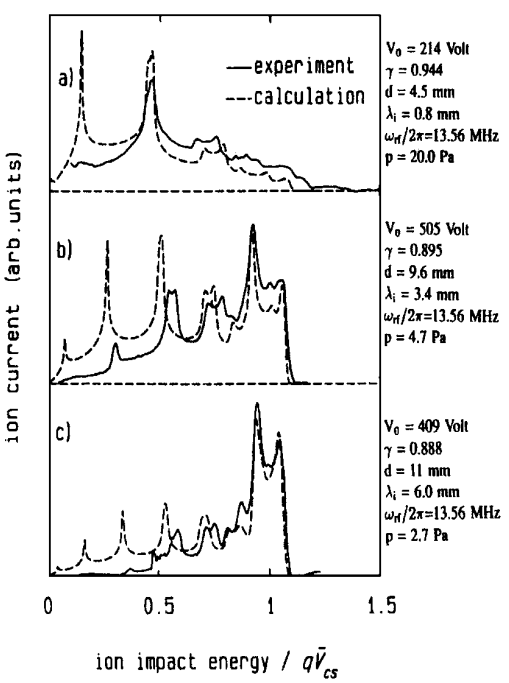

Figure 14. Examples of experimentally and numerically obtained ion energy distributions at the powered electrode. The relevant parameters are given at the right-hand side of each plot. Illustration from [12].

3. Electron energy distribution

The electrons in a RF discharge acquire energy from the oscillating electric field and lose energy mainly in inelastic collisions such as vibrational and electronic excitation and dissociation and ionization of the background gas. The energy loss in elastic collisions is very small due to the small ratio m_e/M, so these collisions almost only lead to a change in momentum and are of importance mainly for the transport coefficients.

The behaviour of the electron energy distribution function in an unmagnetized discharge is described by the Boltzmann equation as

$$\frac{\partial f(\vec{r},\vec{v},t)}{\partial t} + \vec{v}\cdot\vec{\nabla}_{\vec{r}} f(\vec{r},\vec{v},t) - \frac{e}{m}\vec{E}\cdot\vec{\nabla}_{\vec{v}} f(\vec{r},\vec{v},t) = \left(\frac{\partial f(\vec{r},\vec{v},t)}{\partial t}\right)_{coll} \tag{35}$$

which accounts for changes in the density of electrons, f, in a volume element $\mathrm{d}\vec{r}\,\mathrm{d}\vec{v}$ in phase space, due to spatial transport, acceleration, and collisions. Solving this equation is usually simplified by making use of symmetries and the expansion

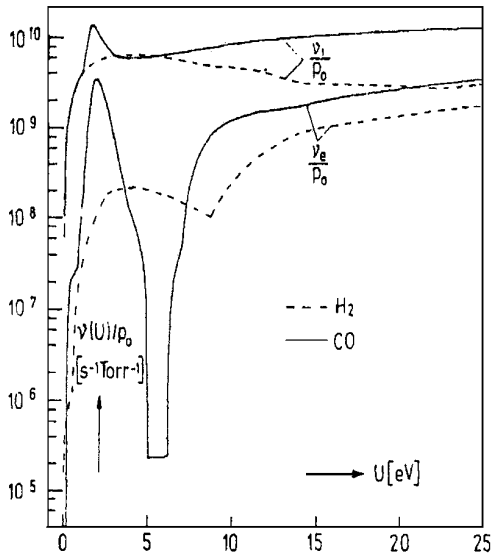

Figure 15. The frequency of the loss of momentum and the energy of electrons in a molecular gas. Note that the energy loss is almost totally covered by the inelastic processes. Illustration from [14].

of f in Legendre polynomials [13]:

$$f(\vec{r},\vec{v},t) = f_0(\vec{r},v,t) + \sum_{k=1}^{\infty} f_k(\vec{r},v,t)P_k(\cos\theta) \qquad (36)$$

where θ is the angle between $\vec{v}$ (the electron velocity) and $\langle\vec{v}\rangle$ (the average velocity). An analysis of the particle and momentum balance in a spherical shell in velocity space and neglection of f_2 and higher-order contributions gives the well known Lorentz approximation for the calculation of f_0, the isotropic part, and $\vec{f}_1$, the anisotropic part:

$$\frac{\partial}{\partial t}f_0 + \frac{v}{3}\vec{\nabla}_{\vec{r}}\cdot\vec{f}_1 + \frac{1}{4\pi v^2}\frac{\partial}{\partial v}[\sigma_E(v) - \sigma_{coll}(v)] = 0 \quad (37a)$$

$$\frac{\partial}{\partial t}\vec{f}_1 + v\vec{\nabla}_{\vec{r}}f_0 - \frac{e\vec{E}}{m}\frac{\partial f_0}{\partial v} + \nu_m\vec{f}_1 = 0 \qquad (37b)$$

$$\sigma_E(v) = -\frac{4\pi}{3}v^2\frac{e\vec{E}}{m}\cdot\vec{f}_1(\vec{r},v,t). \qquad (37c)$$

Here $\sigma_{coll}(v)$ is a function that describes how many electrons are scattered from outside to inside a sphere with radius v in velocity space, so it therefore depends on the specific properties of the background gas.

The distribution function determines important quantities such as the rates for various processes and the transport coefficients (diffusion and mobility). The rate for dissociation, for instance, can be expressed as

$$K_{diss} = 4\pi\int_0^{\infty}\sigma_{diss}(v)vf_0(v)v^2\,\mathrm{d}v \qquad (38)$$

and the diffusion coefficient reads

$$D = 4\pi\int_0^{\infty}\frac{v^2}{3\nu_m}f_0(v)v^2\,\mathrm{d}v. \qquad (39)$$

For the behaviour of the electrons in an RF discharge, the relaxation times and relaxation lengths are important.

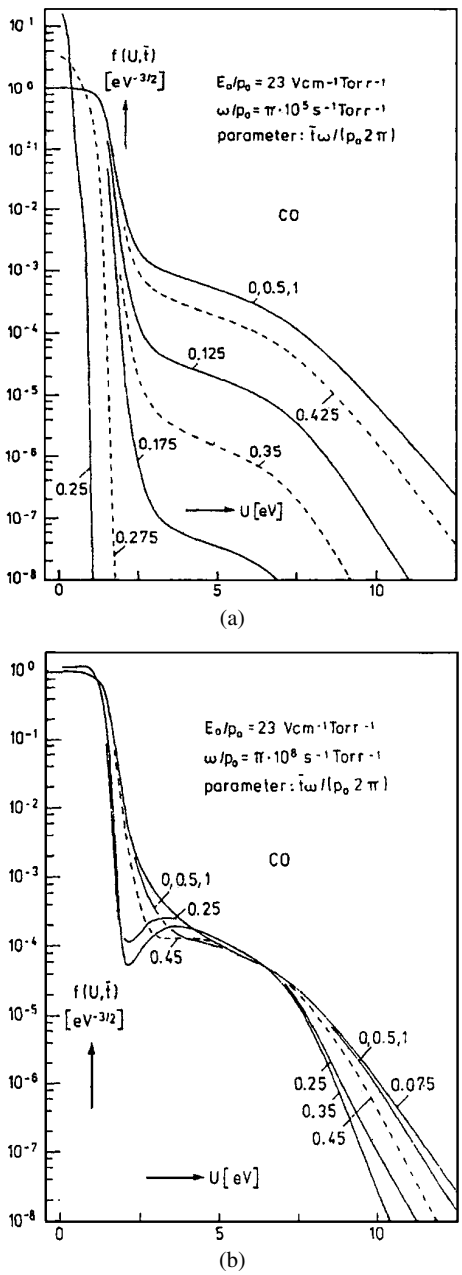

Figure 16. Electron energy distribution in a molecular gas at various phases of the RF cycle, for a low (a) and a high (b) RF frequency. Illustration from [14].

An important quantity for the time-dependent behaviour is the ratio of the RF frequency, ν_{RF}, and the frequency for energy loss, ν_ϵ. The spatial relaxation depends on the ratio between the mean free path for energy loss and the relevant length scales in the discharge.

Let us first consider the time dependence. Figure 15 shows the frequencies for loss of energy and momentum normalized on the pressure, ν_m/p and ν_ϵ/p for a molecular gas, with a peak from vibrational excitation and a tail from dissociation, electronic excitation, and ionization. If the applied normalized RF frequency, ν_{RF}/p, is much lower than both of the loss frequencies, the electron energy distribution function will instantaneously be in equilibrium with the electric field, as in a sequence of dc discharges. On the

other hand, if the RF frequency is much higher than the loss frequencies, the electrons would react to the average electric field. RF discharges are usually operated at frequencies lower than the momentum loss frequency. This means that $\vec{f}_1$ is in equilibrium with the field, but (parts of) f_0, especially in energy ranges where no inelastic collisions occur, are not in equilibrium, because σ_{coll} is related to ν_ϵ. Figure 16 represents the energy distributions at different phases of the RF cycle for low and high frequencies, which illustrates the behaviour discussed [14]. The behaviour of the electrons is shown for a homogeneous discharge, with a time-varying electric field: $E(t) = E_0 \cos(\omega t)$.

Obviously, the rate coefficients for the inelastic processes, especially those involving the high-energy tail of the distribution function, can be affected strongly by the relaxation effects. Often mixtures of gases are used and ν_ϵ may then become significant over the whole energy range, which renders the frequency effects less important.

At low pressures, in particular, the mean free path for the energy loss of the electrons may become very large, even comparable to or exceeding the length of the discharge. In such a case, obviously, the energy distribution function becomes very non-local, as energetic electrons from the sheath can move freely through the quasi-neutral bulk without losing energy. Describing the energy distribution by means of Legendre polynomials in situations with a spatially-varying strong electric field requires much more than the two terms used in the Lorentz approximation [13, 15]. In such cases where the electrons have a mean free path for the energy loss that exceeds the size of the discharge, the distribution function can be described by considering not the kinetic energy, but the total energy; this distribution function is the same everywhere in the discharge; the distribution function in kinetic energy can be found by a simple truncation. In cases where the relaxation times also exceed the RF period, averaging both in space and in time is allowed [16]. Because the kinetic energy reaches its highest value where the potential has a minimum, the reaction rates for inelastic processes, such as the dissociation into radicals, show a maximum at the position where the plasma potential has its highest value. This may lead to an inhomogeneous radical production and, as a consequence, to inhomogeneous particle fluxes.

Let us now consider the heating mechanisms for electrons in an RF discharge in more detail. In the quasi-neutral plasma bulk, the electron motion is governed by the oscillating (usually weak) electric field and collisions with the background gas; their equation of motion is

$$\frac{\mathrm{d}v}{\mathrm{d}t} = -\frac{e}{m} E_0 \exp(\mathrm{i}\omega t) - \nu_m v. \qquad (40a)$$

Assuming a harmonic motion, $(\mathrm{d}/\mathrm{d}t = \mathrm{i}\omega)$, this yields

$$v = -\frac{e}{m(\mathrm{i}\omega + \nu_m)} E_0 \exp(\mathrm{i}\omega t). \qquad (40b)$$

This shows that collisions (equal to resistance) are needed for the electrons to pick up the net power from the field. If the collision frequency is much lower than the driving frequency, the power absorbed over one RF period goes to zero with the collision frequency. At collision frequencies much larger than the RF frequency, the current density and the electric field are in phase and the quasi-neutral bulk behaves as a resistor. This condition corresponds to neglecting the time derivative of the anisotropic part of the distribution function in equation (37*b*), as discussed above. Usually, the collision frequency is much higher than the driving frequency in RF discharges, except at low pressures, with frequencies in the VHF range.

Electrons outside the quasi-neutral bulk may also be heated by the oscillating sheath front. Two mechanisms play a role, stochastic heating and wave-riding. Stochastic heating reflects the change in energy when the electrons are bouncing between the sheaths. Because of the high electric field, the sheath can be considered as an impenetrable wall and, if the sheath expands or contracts fast enough, the electrons will gain or loose some momentum and the electron energy will also be changed. The effect of these 'collisions' with the sheath boundary is a random walk in energy, leading to a diffusion in the energy space from low to high energies because of the sign of the gradient of the distribution function [4, 16].

In the sheath, the electrons are pushed away into the bulk when the sheath expands. At high frequencies and high pressures, the expansion velocity is so large that the electrons cannot react instantaneously (high pressure implies a low mobility) and become accelerated only when the electric field has reached a sufficiently high value. The electrons 'ride' on the boundary of the expanding sheath. This leads to a combination of a high electron current and a high electric field in the zone between the quasi-neutral centre and the sheath and, as a consequence, to a significant ohmic heating [4].

A separate group of electrons are the so-called secondary electrons. They are released from the electrode surface by the incoming ions. Typical probabilities are 1%. These electrons are accelerated by the field in the space charge sheath. If both the field and the pressure are high enough, they can ionize within the sheath, and an avalanche may be created. A significant part (to practically 100%) of the ionization may then be due to these secondary electrons. Thus, when the power is increased, the discharge may move from a situation that is dominated by the bulk properties (α regime) to a situation that is dominated by secondary electrons (γ regime) [17].

4. Concluding remarks

In a lecture of 90 minutes many aspects and details of RF discharges have to remain undiscussed and the few references below are only a very small part of the vast amount of literature available. For further study I would recommend the books [4] and [18].

References

[1] Manos D M and Flamm D L (eds) 1988 *Plasma Etching, An Introduction* (San Diego, CA: Academic)

[2] Bruno G, Capezzuto P and Madan A (eds) 1995 *Plasma Deposition of Amorphous Silicon-Based Materials* (San Diego, CA: Academic)

[3] Williams P F (ed) 1997 *Plasma Processing of Semiconductors (NATO ASI Series E: Applied Sciences vol 336)* (Dordrecht: Kluwer)

[4] Lieberman M A and Lichtenberg A J 1994 *Principles of Plasma Discharges and Materials Processing* (New York: Wiley)
[5] van Roosmalen A J, Baggerman J A G and Brader S J H 1991 *Dry Etching for VLSI* (New York: Plenum)
[6] Meijer P M and Goedheer W J 1991 *IEEE Trans. Plasma Sci.* **19** 170–5
[7] Goedheer W J, Meijer P M, Bezemer J, Passchier J D P and van Sark W G J H M 1995 *IEEE Trans. Plasma Sci.* **23** 644–9
[8] Rauf S and Kushner M J 1998 *J. Appl. Phys.* **83** 5087–94
[9] Benoit-Cattin P and Bernard L-C 1968 *J. Appl. Phys.* **39** 5723–6
[10] Wild C and Koidl P 1989 *Appl. Phys. Lett.* **54** 505–7
[11] Manenschijn A and Goedheer W J 1991 *J. Appl. Phys.* **69** 2923–30
[12] Manenschijn A, Janssen G C A M, van der Drift E and Radelaar S 1991 *J. Appl. Phys.* **69** 1253–62
[13] Winkler R, Wilhelm J and Hess A 1983 *Beitr. Plasmaphys.* **23** 483–96
[14] Winkler R, Capitelli M, Dilonardo M, Gorse C and Wilhelm J 1986 *Plasma Chem. Plasma Proc.* **6** 437–56
[15] Winkler R, Braglia G L and Wilhelm J 1989 *Ann. Phys., Lpz.* **46** 21–40
[16] Kaganovitch I D and Tsendin L D 1992 *IEEE Trans. Plasma Sci.* **20** 66–75
[17] Godyak V A, Piejak R B and Alexandrovich B M 1992 *Phys. Rev. Lett.* **68** 40–3
[18] Raizer Y P, Shneider M N and Yatsenko N A 1995 *Radio-Frequency Capacitive Discharges* (Boca Raton, FL: CRC Press)